Journal of Nuclear Materials 520 (2019) 87–95

Contents lists available at ScienceDirect

Journal of Nuclear Materials

journal homepage: www.elsevier.com/locate/jnucmat

Thermal analysis of projected molten salt compositions during FFTF and EBR-II used nuclear fuel processing

Toni Y. Karlsson [a], Guy L. Fredrickson [a, *], Tae-Sic Yoo [a], DeeEarl Vaden [a], Michael N. Patterson [b], Vivek Utgikar [c]

[a] Pyrochemistry and Molten Salt System Department, Idaho National Laboratory, Idaho Falls, ID, USA
[b] Materials and Fuels Complex Production Facilities, Idaho National Laboratory, Idaho Falls, ID, USA
[c] Department of Chemical and Materials Engineering, University of Idaho, Moscow, ID, USA

ARTICLE INFO

Article history:
Received 19 December 2018
Received in revised form
8 April 2019
Accepted 8 April 2019
Available online 10 April 2019

Keywords:
Electrorefining
Electrorefiner
Eutectic
LiCl–KCl
Molten salt
Nuclear fuel
Uranium
Liquidus

ABSTRACT

This work examines the change in liquidus temperature of the salt used in the Mk-IV electrorefiner at the Idaho National Laboratory during processing campaigns of sodium-bonded driver fuels from Experimental Breeder Reactor II and the Fast Flux Test Facility reactor. Modeling and Simulation Tool for Electrochemical Recycling Systems (MASTERS), an INL proprietary pyroprocessing flowsheet simulation tool, was used to simulate the processing campaigns and determine the resulting composition changes of the Mark-IV electrorefiner salt. Surrogate salt samples simulating the Mk-IV electrorefiner salt during the fuel processing campaigns were prepared, and the thermal properties were measured via differential scanning calorimetry. Results from this study indicate that after processing approximately 2,150 kg of uranium metal from used fuel, the liquidus temperature of the molten salt exceeds 520 °C, which is a significant increase from 352 °C (the melting temperature of eutectic LiCl–KCl). It was also found that the liquidus temperature is strongly dependent on the amount of NaCl accumulating in the Mk-IV electrorefiner salt. Thus, the assessment of the liquidus temperature during the subsequent fuel processing campaigns can be simplified by considering the ternary LiCl–KCl–NaCl system only.

© 2019 Elsevier B.V. All rights reserved.

1. Introduction

The mission of the U.S. Department of Energy (DOE) Integral Fast Reactor (IFR) Program was to demonstrate a closed nuclear fuel cycle using pyroprocessing on Experimental Breeder Reactor II (EBR-II) at the Argonne National Laboratory – West (ANL-W). EBR-II was a sodium-cooled fast reactor fueled with sodium-bonded metallic driver and blanket fuels [1]. The pyroprocessing line was co-located next to EBR-II in the Fuel Cycle Facility (FCF) hot cells. However, changing priorities within the DOE resulted in the shutdown of EBR-II in 1994, effectively terminating the IFR program before pyroprocessing was demonstrated as a fuel-cycle technology [2]. Attentions then focused on finding a disposition path for the inventories of used driver and blanket fuels, approximately 3 and 22 MT, respectively. After the shutdown of EBR-II, several major changes occurred in succession.

The Spent Fuel Treatment (SFT) Program was initiated to treat the inventories of used sodium-bonded metallic fuels for disposition. In accordance with the new mission, the Fuel Cycle Facility was renamed the Fuel Conditioning Facility, maintaining its three letter acronym, FCF. Following a review of competing technologies, pyroprocessing was selected as the means of treating the used fuels.[1] The pyroprocessing line designed for the IFR Program was modified to accommodate the new SFT Program.[2] The SFT Demonstration Project was performed in FCF from June 1996 to August 1999 to verify the effectiveness of the pyroprocessing technology [3,4]. In September 2000, the DOE issued a Record of Decision selecting pyroprocessing as the preferred treatment

[1] Sodium metal is highly reactive, particularly with water. As a result, in order to meet the acceptance criteria of a geologic repository, sodium-bonded metallic fuels require treatment to deactivate the sodium.

[2] The IFR pyroprocessing was designed to process used driver fuel into new driver fuel. The SFT pyroprocessing is designed to process used driver and blanket fuels into materials suitable for disposition.

* Corresponding author. Pyrochemistry and Molten Salt System Department Idaho National Laboratory, P.O. Box 1625, Idaho Falls, ID, 83415-6188, USA.
E-mail address: guy.fredrickson@inl.gov (G.L. Fredrickson).

https://doi.org/10.1016/j.jnucmat.2019.04.016
0022-3115/© 2019 Elsevier B.V. All rights reserved.

Abbreviations

ASME	American Society of Mechanical Engineers
EBR-II	Experimental Breeder Reactor II
DFI	Driver Fuel Initiative
DSC	Differential Scanning Calorimeter
DU	Depleted Uranium
FCF	Fuel Cycle Facility (early name)
FCF	Fuel Conditioning Facility (present name)
FFTF	Fast Flux Test Facility (a Hanford reactor)
Fs	Fissium Alloy
HEU	High Enriched Uranium
HM	Heavy Metal (typically the actinide content)
ICPP	Idaho Chemical Processing Plant
IFR	Integral Fast Reactor
INEEL	Idaho National Engineering and Environmental Laboratory
INL	Idaho National Laboratory
INTEC	Idaho Nuclear Technology and Engineering Center
LCC	Liquid Cadmium Cathode
LEU	Low Enriched Uranium
MASTERS	Modeling and Simulation Tool for Electrochemical Recycling Systems
MFC	Materials and Fuels Complex
Mk-IV ER	Mark-IV Electrorefiner
MTG	Mass Tracking System
RCRA	Resource Conservation and Recovery Act
REDOX	Reduction/Oxidation
TGA	Thermogravimetric Analyzer
TRU	Transuranic
DOE	Department of Energy

option for sodium-bonded metallic fuels [5]. In 2005, management of ANL-W was transferred from the University of Chicago to Battelle Energy Alliance, and ANL-W was renamed the Materials and Fuels Complex (MFC). At the same time, MFC was consolidated into the Idaho National Engineering and Environmental Laboratory (INEEL), and the INEEL was renamed the Idaho National Laboratory (INL).

EBR-II, as the name implies, was an experimental reactor. As such, it used different types (formulations) of driver fuels during its history. These are generally referred to as Mk-I through Mk-V fuels, though the details are more complex. This work focuses on two types of EBR-II driver fuel: Mk-II and Mk-III. The Mk-II is high enriched uranium (HEU) with 5 wt% fissium alloy (i.e., U5Fs).[3] And the Mk-III is HEU with 10 wt% zirconium (i.e., U10Zr). The Mk-III and later fuel types were specifically designed to support the IFR Program. Earlier fuel types were pre-IFR concept. All EBR-II blanket fuel was fabricated from depleted uranium (DU).

The Fast Flux Test Facility (FFTF) Reactor at the Hanford Site was a sodium-cooled fast reactor fueled with both mixed oxide (MOX) and sodium-bonded metallic driver fuels. It too was an experimental reactor. The FFTF shutdown preceded the EBR-II shutdown by about 2 years. The inventory of used sodium-bonded metallic fuel (248.1 kg HM) was shipped to the INL for processing in FCF. The composition of this fuel was similar to the EBR-II Mk-III fuel.

A schematic of the SFT pyroprocessing flowsheet is shown in Fig. 1. It is different from the IFR pyroprocessing flowsheet in several distinct ways. The IFR flowsheet was designed for reprocessing; the SFT flowsheet is designed for used fuel treatment and disposition. The IFR flowsheet included fuel fabrication equipment; the SFT flowsheet is truncated at the casting furnace. The IFR flowsheet included a driver fuel element chopper and the Mk-IV electrorefiner (ER); the SFT flowsheet includes an additional blanket fuel element chopper and the Mk-V ER.[4] The IFR flowsheet recovered electrorefined uranium as high enriched uranium (HEU); the SFT flowsheet recovers electrorefined uranium as low enriched uranium (LEU).[5] The IFR flowsheet had means of recovering transuranics as a uranium alloy; the SFT flowsheet allows the transuranics to remain in the salt and follow the disposition path of the salt.

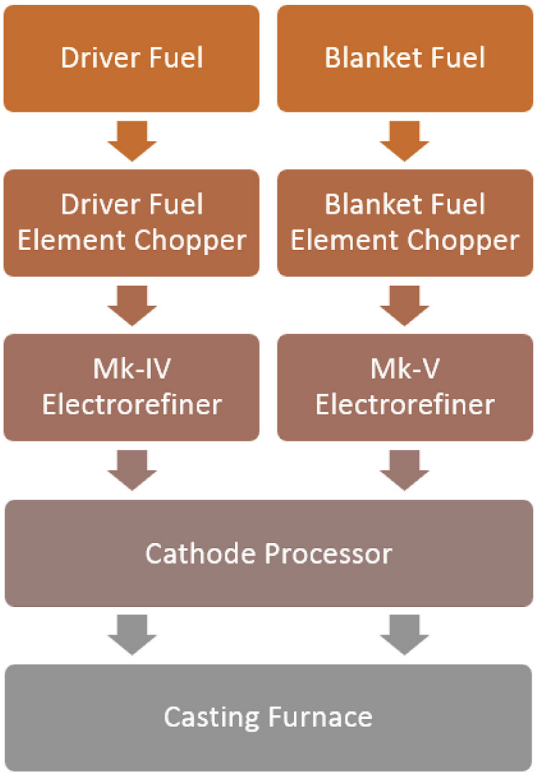

Fig. 1. Schematic of the SFT pyroprocessing flowsheet.

Between 1996 and 2010, FCF processed both EBR-II blanket fuel and Mk-III driver fuel that were located at MFC. In 2010, the decision was made to focus resources on driver fuel processing and the name "SFT Program" was dropped in favor of the name "Driver Fuel Initiative (DFI) Program" to emphasis the new focus. In 2011, FCF processed most of the FFTF driver fuel (218.8 kg HM); the remaining inventory was preserved for research purposes and will be processed at a later date. And from 2013 to present, FCF has processed EBR-II Mk-II driver fuel. The inventory of this particular driver fuel was transferred from ANL-W to the Idaho Chemical Processing Plant (ICPP) in the 1970s for aqueous reprocessing. However, the inventory remained in the fuel storage water pool when

[3] The nominal composition of fissium is 2.4 Mo, 1.9 Ru, 0.3 Rh, 0.2 Pd, 0.1 Zr, and 0.01 Nb, wt% [6,7].

[4] In the SFT flowsheet, the Mk-IV ER is dedicated to driver fuel and the Mk-V ER is dedicated to blanket fuel. Separate choppers are required because the driver fuel elements are significantly smaller than the blanket fuel elements.

[5] HEU is uranium with >20% U235; LEU is uranium with <20% U235. The safeguards requirements of LEU are more relaxed than HEU. There are many reactor technologies that can use LEU.

reprocessing operations at ICPP were shutdown in 1992. The location of ICCP is now named the Idaho Nuclear Technology and Engineering Center (INTEC), and current research activities focus on used fuel storage. Since 2013, the Mk-II driver fuel has been retrieved from the water pool, transferred by cask-shipment to MFC, and processed in FCF.

The present investigation was performed in 2010 in preparation of pyroprocessing FFTF and EBR-II Mk-II fuels. For obvious reasons, it is important to understand and characterize the factors that affect the useful life of the molten salt in an electrorefiner. Such factors include increasing decay heat load from the accumulation of fission products, increasing fissile inventory load from the accumulation of actinides, and increasing liquidus temperature from the accumulation of fission products, actinides, and bond-sodium. The purpose of the present investigation was twofold. Predict, by process modeling, how the composition of the Mk-IV ER salt will change as batch-by-batch of FFTF and EBR-II Mk-II driver fuel are processed. Determine, by laboratory study, how the predicted composition change affects the liquidus temperature of the salt.

The DFI pyroprocess recovers electrorefined uranium as LEU (target of 19.5% U235) from the HEU driver fuels (nominally 63–75% U235). During electrorefining, the fuel is anodically dissolved from a steel basket, while electrorefined uranium is cathodically deposited onto a steel mandrel. The purity of the electrorefined metal is typically >99.5 wt% uranium [8]. Active metals in the used fuel, such as the bond sodium, transuranics, and the alkali, alkaline earth, and lanthanide fission products accumulate in the salt with each batch of fuel processed [9]. Less active metals, mostly the transition metal fission products and fuel element cladding, remain undissolved in the anode basket [10–13].

Consequently, the salt in the Mk-IV ER is a complex mixture of many metal chloride species. The primary component is LiCl–KCl (58-42 mol%) eutectic salt, that has a melting temperature of $352 \pm 5\,^{\circ}C$. The Mk-IV ER is operated at 500 °C, with a nominal salt inventory of approximately 470 kg. The UCl_3 concentration is typically maintained between 4 and 8 wt% to support transport of uranium from the anode to the cathode and to support the accumulation of active metals in the salt [14]. As the active metals accumulate in the salt, they do so at the expense of the UCl_3 concentration according to redox reactions between the active metals and the salt. In the following reaction, Me(s) is an active metal in the fuel, and U(s) is the uranium reduced from the salt.

$$\frac{x}{3}UCl_3 + Me(s) \rightleftharpoons MeCl_x + \frac{x}{3}U(s)$$

The reduced uranium will deposit onto any metallic surface in electrical contact with the anode basket, after which it is ultimately electrorefined to the cathode. A typical anode basket loading of chopped fuel contains a sufficient quantity of active metals to displace about 1 kg of uranium from the salt [9]. The UCl_3 concentration is maintained by adding $CdCl_2$ to the salt as necessary while metallic uranium is present in the vessel. The $CdCl_2$ oxidizes the metallic uranium to form UCl_3, and the reduced metallic cadmium accumulates in the bottom of the ER vessel [14,15].

$$3CdCl_2 + 2U(s) \rightleftharpoons 2UCl_3 + 3Cd(l)$$

2. Modeling the electrorefiner salt composition

2.1. Modeling objectives

The campaign to process FFTF driver fuel was completed (27 batches) in 2011. And beginning in 2013, a significantly larger campaign to process EBR-II Mk-II driver fuel was initiated (projected to be approximately 165 batches for modeling purposes). The major components of FFTF and EBR-II Mk-II fuels are listed in Table 1. The composition of FFTF fuel is U10Zr (wt%) [6]. The composition of EBR-II Mk-II fuel is U5Fs (wt%) [6,7]. Prior to the FFTF fuel campaign, the Mk-IV ER processed mostly EBR-II Mk-III driver fuel, which was U10Zr (wt%), and a small quantity of EBR-II blanket fuel.[6]

Table 1
FFTF and EBR-II Mk-II fuel inventories.

Component	FFTF, kg	EBR-II Mk-II, kg
Total U[a]	220	1939
TRU	7	9
Zirconium	32	–
Sodium	7	53
Other Elements	7	43
Total Fuel Mass	273	2044

[a] Ta. Total U is the sum of U-235 and U-238otal U is the sum of U-235 and U-238.

In 2010, MASTERS (Modeling and Simulation Tool for Electrochemical Recycling Systems) [16] was used to predict the composition of the salt throughout the planned fuel processing campaigns (27 batches of FFTF fuel, and 165 batches of EBR-II Mk-II fuel). MASTERS is proprietary software for pyroprocessing flowsheet modeling developed at INL. The historic (pre-FFTF fuel processing) and projected (post-FFTF fuel processing) composition of the Mk-IV ER salt are shown in Fig. 2.

MASTERS simulation predicted that the salt composition would change significantly, with ever increasing concentrations of fission products and bond-sodium, during the course of the FFTF fuel and EBR-II Mk-II fuel processing campaigns. An obvious consequence of these findings was concern for their impact on the thermal properties of the salt. The effect on liquidus temperature was of particular concern. If the operating temperature of the salt is above its liquidus temperature, the salt exists as a single molten phase. If the operating temperature of the salt is below its liquidus temperature, the salt exists in two or more phases, which typically include a molten phase and one or more solid phases. Liquids temperature is a function of the phase behavior of the salt, which is to say the composition of the salt. The term *super heat* is used to describe the difference between the operating temperature and the liquidus temperature. For example, if the operating temperature is 500 °C, and the liquidus temperature is 360 °C, the super heat is 140 °C.

The concern for operations of the Mk-IV ER was that at some point while processing the 165 batches of EBR-II Mk-II fuel that, in order to maintain a minimum superheat of 75 °C, it would be necessary to remove salt from the ER and replace it with LiCl–KCl eutectic salt. To address this concern, investigation of the thermal properties of the LiCl–KCl salt with the projected active metal accumulations from the planned FFTF and EBR-II Mk-II fuel processing campaigns was conducted.

2.2. Modeling methods

This study focused on the processing 27 batches of FFTF fuel and 165 batches of EBR-II Mk-II fuel, for a total of 192 batches of spent driver fuel processed in the Mk-IV ER. The projected salt compositions were based on the MASTERS simulation results. The five

[6] Historically, a small amount of EBR-II blanket fuel was processed in the Mk-IV ER for various reasons (testing, decreasing the enrichment of the salt, etc.). However, the Mk-V ER has only processed blanket fuel.

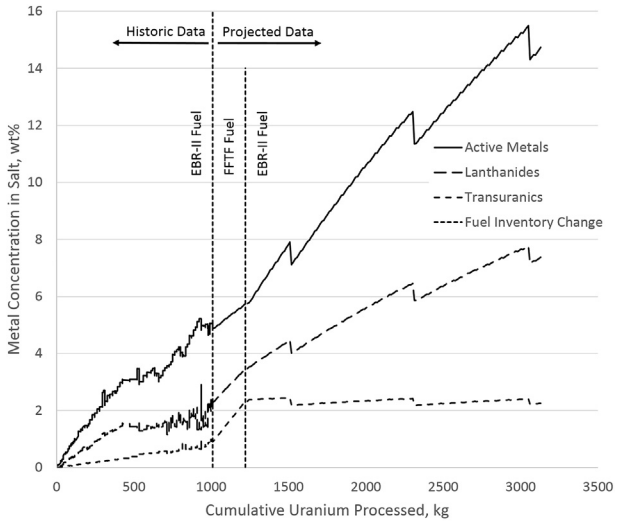

Fig. 2. MASTERS estimation of Mk-IV ER salt compositions during processing of FFTF and EBR-II driver fuels. Active metals include bond-sodium and the alkali and alkaline earth fission products.

most significant process assumptions adopted for the simulation are summarized in Table 2. And the five most significant process conditions constraining the operation of the electrorefiner are summarized in Table 3.

During the FFTF and EBR-II fuel processing simulation, MASTERS predicted violations of all five operating conditions listed above. During FFTF fuel processing, Condition 1 was violated five times. During EBR-II Mk-II fuel processing, Condition 1 was violated 45 times and Conditions 3 and 4 were each violated three times. The sudden decreases in concentrations that occur in Fig. 2 at approximately 1500, 2300, and 3050 kg uranium processes, are due to violations of Condition 4. Each time, 50 kg of fresh LiCl–KCl eutectic salt was added to the ER vessel (according to the rules in Table 3). The MASTERS simulation ran 27 batches of FFTF fuel, and 165 batches of EBR-II Mk-II fuel, for a total of 192 batches of fuel. The nine salt compositions selected for study are listed in Table 4. The compositions are based on the MASTERS simulation results. Column titles in Table 4 represent the fuel source and batch number. For example, EBR-II B100 refers to the 100th batch of EBR-II Mk-II fuel (following the 27th batch of FFTF fuel).

Prior to the FFTF fuel processing, the Mk-IV ER salt composition was dominated by the following thirteen metal chlorides, which accounted for >99% of the salt mass: LiCl, KCl, NaCl, CsCl, $SrCl_2$, $BaCl_2$, $LaCl_3$, $CeCl_3$, $PrCl_3$, $NdCl_3$, $SmCl_3$, UCl_3, and $PuCl_3$ [17]. The MASTERS simulation results confirmed that these same metal chlorides continue to dominate the salt composition while processing the entire inventories of FFTF and EBR-II Mk-II fuels. Therefore, these thirteen metal chlorides were selected to serve as the basis for formulating the simulant salt compositions. However, to allow the simulant salts to remain non-radiological and free of Resource Conservation and Recovery Act (RCRA) metals, $GdCl_3$ was used as a surrogate for the actinide chlorides (UCl_3 and $PuCl_3$) and $SrCl_2$ was used as a surrogate for $BaCl_2$. Therefore, the simulant salts were formulated from eleven metal chlorides. The compositions of the simulant salts are listed in Table 5. Information regarding the source and purity of the reagent chemicals used to formulate the simulant salts are summarized in Table 6.

3. Experimental methods

The simulant salts were prepared in a glovebox with the oxygen and moisture concentrations maintained below 0.1 ppm. After weighing the individual salts (Mettler, MS3045/03, ±0.0005 g), the ingredients were combined in a 30 mL nickel crucible with a nickel lid, and the crucible heated to 600 °C in a furnace (Thermo Scientific) for 1 h. At 600 °C, the salt mixture was completely molten and there were no visual indications of reaction with the nickel crucible. The crucible was removed from the furnace and cooled while inside the glovebox. To ensure a homogenous sample, the entire salt mixture was pulverized using a mortar and pestle and sieved to yield a powder with particle size of 100% passing 150 μm.

In preparation for the simulant salt experiments, the LiCl–KCl phase diagram was studied and compared to the work of others. This was done to confirm the validity of experimental procedures and the accuracy of the thermal measurement techniques and

Table 2
Summary of process assumptions used in MASTERS.

Assumption Number	Process Assumptions Made in the MASTERS Modeling Code
1	Each batch of FFTF fuel contained 11.6 kg HM, and each batch of EBR-II Mk-II fuel contained 12.0 kg HM.
2	Each batch took 15 days to process.
3	Residual salt adhering to the electrorefined uranium product harvested from the ER was returned to the ER.
4	Residual salt adhering to the anode residue (fuel element hardware, noble metal fission products, and undissolved fuel) harvested from the ER was not returned to the ER. This residual salt reported to the salt waste stream.
5	Anode residue (fuel element hardware and noble metal fission products) are inert to the electrorefining process. Anode residue reported to the metal waste stream.
6	95% of the uranium in the anode basket was transported to the cathode. The remaining 5% of the uranium stayed with the anode residue and reported to the metal waste steam

Table 3
Summary of process conditions used in MASTERS.

Condition Number	Conditions that Constrain the Operation of the Mk-IV ER in the MASTERS Modeling Code
1	The uranium concentration in the salt must remain above 5 wt%. If the uranium concentration drops below 5 wt%, cadmium chloride ($CdCl_2$) is added to increase the uranium concentration.
2	The fissile material inventory in the salt must remain below 77.2 kg. If the fissile inventory exceeds 77.2 kg, then 50 kg of salt is removed from the ER.
3	The total-Pu-equivalent inventory must remain below 10 kg. If the total-Pu-equivalent inventory exceeds 10 kg, then 50 kg of salt is removed from the ER.
4	The total salt mass in the ER must remain above 430 kg. If the total salt mass drops below 430 kg, then 50 kg of eutectic LiCl–KCl salt is added.
5	The total salt mass in the ER must remain below 550 kg. If the total salt mass exceeds 550 kg, then 50 kg of salt is removed from the ER.

Table 4
Compositions, wt%, of Mk-IV ER salts for select batches.

Element	FFTF B1	FFTF B27	EBR-II B25	EBR-II B50	EBR-II B75	EBR-II B100	EBR-II B125	EBR-II B150	EBR-II B165
Chlorine	60.5	58.3	58.1	57.9	57.1	56.8	56.8	56.1	55.0
Potassium	21.8	19.8	19.0	17.4	15.9	15.7	14.3	13.1	13.1
Lithium	5.6	5.1	4.9	4.5	4.1	4.1	3.7	3.4	3.4
Uranium	4.5	4.9	5.5	6.2	5.3	5.4	6.1	5.2	5.9
Sodium	3.2	3.6	4.4	5.8	7.0	7.3	8.4	9.4	9.0
Neodymium	1.0	2.2	1.8	2.2	2.6	2.7	3.0	3.4	3.2
Cesium	1.0	1.6	1.3	1.6	1.9	2.0	2.2	2.5	2.4
Plutonium	0.8	1.1	2.0	2.1	2.2	2.0	2.1	2.2	2.0
Cerium	0.6	0.9	1.0	1.2	1.5	1.5	1.7	1.9	1.8
Lanthanum	0.3	0.5	0.5	0.7	0.8	0.8	0.9	1.0	1.0
Praseodymium	0.3	0.4	0.5	0.6	0.7	0.8	0.9	1.0	0.9
Samarium	0.3	0.4	0.4	0.5	0.6	0.6	0.6	0.7	0.7
Barium	–	–	0.4	0.6	0.9	1.0	1.2	1.4	1.3
Strontium	0.2	0.2	0.3	0.3	0.4	0.4	0.5	0.6	0.5

Table 5
Compositions, wt%, of the simulant salts.

Chloride	FFTF B1	FFTF B27	EBR-II B25	EBR-II B50	EBR-II B75	EBR-II B100	EBR-II B125	EBR-II B150	EBR-II B165
LiCl	34.82	31.96	29.91	26.89	24.79	24.29	21.83	20.15	20.31
KCl	42.02	38.43	36.27	32.51	29.98	29.39	26.42	24.39	24.59
NaCl	8.303	9.373	11.23	14.36	17.57	18.29	20.67	23.34	22.59
CsCl	1.241	1.981	1.603	1.988	2.385	2.443	2.730	3.053	2.944
$SrCl_2$	0.343	0.381	1.151	1.713	2.271	2.487	2.914	3.379	3.314
$LaCl_3$	0.563	0.853	0.956	1.166	1.387	1.417	1.581	1.766	1.704
$CeCl_3$	0.984	1.519	1.728	2.143	2.567	2.637	2.953	3.311	3.191
$PrCl_3$	0.499	0.774	0.875	1.074	1.289	1.321	1.473	1.653	1.594
$NdCl_3$	1.821	1.985	3.086	3.766	4.479	4.577	5.102	5.703	5.492
$SmCl_3$	0.390	0.658	0.696	0.825	0.956	0.964	1.059	1.172	1.119
$GdCl_3$	9.017	12.09	12.49	13.56	12.33	12.19	13.27	12.07	13.15

Table 6
List of the reagent chemicals.

Chemical Name	Chemical Formula	Supplier	Purity, %	Form
Cerium (III) Chloride	$CeCl_3$	Sigma Aldrich	≥99.99	Anhydrous Beads, 10 mesh
Cesium Chloride	CsCl	Sigma Aldrich	99.99	Anhydrous Beads, 10 mesh
Gadolinium (III) Chloride	$GdCl_3$	Sigma Aldrich	99.99	Anhydrous
Lanthanum (III) Chloride	$LaCl_3$	Alfa Aesar	99.999	Ultra-Dry Powder
Lithium Chloride	LiCl	Sigma Aldrich	99.999	Anhydrous Beads, 10 mesh
Eutectic Lithium Chloride/Potassium Chloride	LiCl–KCl	Sigma Aldrich	99.99	Anhydrous Beads
Neodymium (III) Chloride	$NdCl_3$	Sigma Aldrich	≥99.99	Anhydrous Powder
Potassium Chloride	KCl	Sigma Aldrich	99.999	Anhydrous Beads, 10 mesh
Praseodymium (III) Chloride	$PrCl_3$	Sigma Aldrich	99.99	Anhydrous Powder
Samarium (III) Chloride	$SmCl_3$	Alfa Aesar	99.9	Ultra-Dry Powder
Sodium Chloride	NaCl	Sigma Aldrich	99.999	Anhydrous Beads
Strontium (II) Chloride	$SrCl_2$	Sigma Aldrich	≥99.99	Anhydrous Powder

instrumentation. For the LiCl–KCl study, eight LiCl–KCl salts of varying compositions from 0 to 100 mol% LiCl were prepared in the same manner as the simulant salts.

Thermal properties (onset temperatures, liquidus temperatures, and enthalpies of fusion and crystallization) of the LiCl–KCl binary salts and the simulant salts were measured using a differential scanning calorimeter (DSC) thermogravimetric analyzer (TGA) (Netzsch, STA 449 F3). Because LiCl is extremely hygroscopic, DSC sample preparation was performed in the argon-atmosphere glovebox. Salt samples, approximately 10 mg each, were loaded into a gold-coated, stainless-steel crucibles. The crucible assembly consisted of three gold-coated parts: lid, seal, and pan. The salt was loaded into the pan, the seal was placed on top of the pan, and the lid tightened with a torque driver (2.5 N•m) to seat the seal between the pan and lid. Once sealed, all surfaces in contact with the salt samples were gold-coated. The sealed crucibles were transferred out of the glovebox and into the DSC instrument. DSC samples were run using the parameters shown in Table 7. Each salt sample was subject to three thermal cycles (heating and cooling) during the DSC measurements.

4. Results

4.1. LiCl–KCl phase diagram

The LiCl–KCl phase diagram in Fig. 3a was constructed using the experimental values obtained in this work and compared to the work of others including Zemczuzny and Rambach [18], Richards and Meldrum [19], Elchagardus and Laffite [20], Korin and Soifer [21], Basin et al. [22]. The thermal data points obtained in this research lie within ±5 °C of other reported liquidus and eutectic temperatures.

Table 7
DSC operating parameters.

Parameter	Setting
Crucible Material	Au-Plated Stainless Steel
Crucible Sealing Torque	2.5 N m
Purge Gas Flow Rate	20 cm^3 min^{-1}
Protective Gas Flow Rate	20 cm^3 min^{-1}
Furnace Atmosphere	Argon
Furnace Material	Platinum Furnace (0–600 °C)
Sample Carrier Material	Platinum/Rhodium
Thermocouple Type	Type S
Calibration	Temperature, Sensitivity
Heating/Cooling Rate	10 K min^{-1}, 2 K min^{-1}
Sample Size	10 ± 1 mg

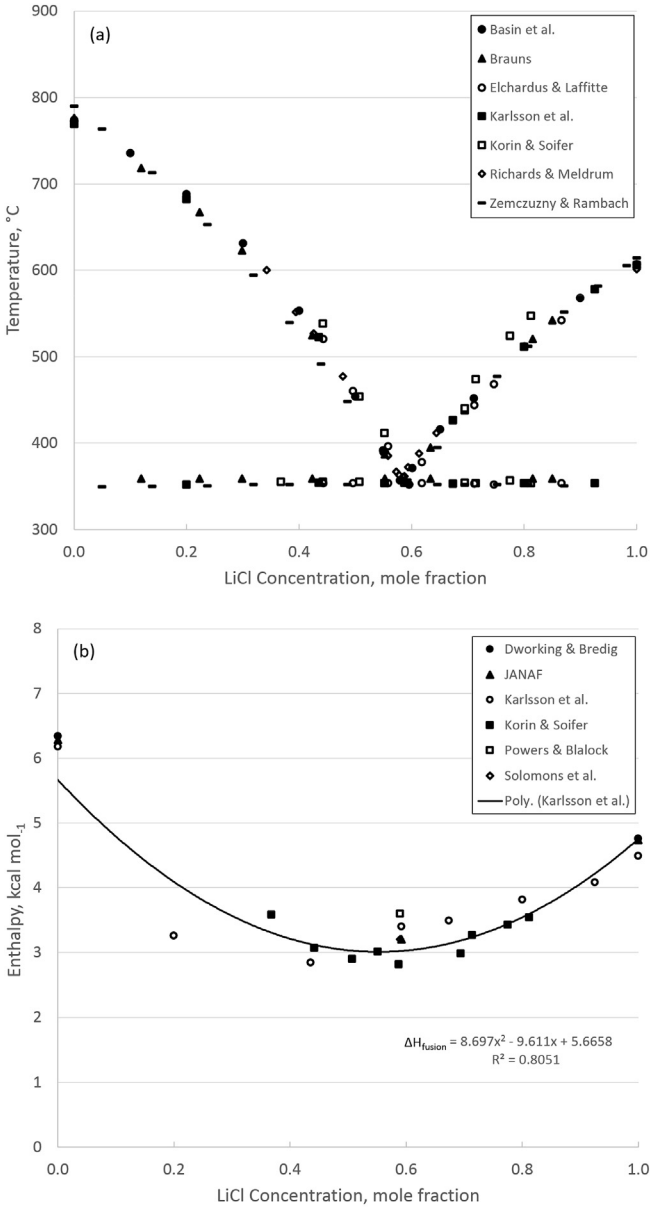

Fig. 3. (a) LiCl–KCl binary phase diagram and (b) enthalpy of fusion for the LiCl–KCl binary system.

An approximation of the system enthalpy is illustrated in Fig. 3b. The thermal data used for this approximation were taken from DSC cooling curves with a cooling rate of 10 K min^{-1}. The DSC cooling curves, rather than heating curves, were used because the molten salt is in better contact with the surface of the DSC crucible, which allows for more accurate enthalpy measurements. The enthalpy calculations assume atmospheric pressure and agree well with literature data [21,23–26]. The equation for the enthalpy of fusion, ΔH_{fusion}, is based on a polynomial fit of the data in Fig. 3b.

4.2. Thermal properties of the simulated salts

To serve as an example, a series of three repetitive DSC thermograms are shown in Fig. 4 for EBR-II B100 simulant salt. The heating rate for each thermogram was 10 K min^{-1}. Each peak along the curves represents a thermal response of the sample to heating, and the overlap of the three curves is an indication of the repeatability of the measurements. Peak A represents the onset temperature; temperature where phase transitions begin; beginning of the first peak in a DSC thermogram. Peak F represents the liquidus temperature; temperature beyond which the sample is entirely molten and no further phase transitions occur; end of the last peak in a DSC thermogram. Peaks B through E represent other phase transitions in the salt that were not identified; the liquidus temperature behavior was of primary interest.

The number and complexity of the peaks in the DSC thermograms were observed to increase in simulant salts containing higher amounts of impurity chlorides. For example, the thermograms of EBR-II B25, EBR-II B100 (see Fig. 4), and EBR-II B165 contained two, four, and five peaks, respectively. This clearly suggests that the latter contains a higher number of phases, transitions, and/or chemical species. Identifying the cause of thermal features between the onset temperature and the liquidus temperature was beyond the scope of this study. The measurements of onset and liquidus temperatures were only slightly affected by variations to DSC heating rates; these data are not presented here.

The onset temperature, liquidus temperature, and impurity concentration (alkali, alkaline earth, and lanthanide fission products, transuranics, and sodium-bond) of the nine simulant salts are

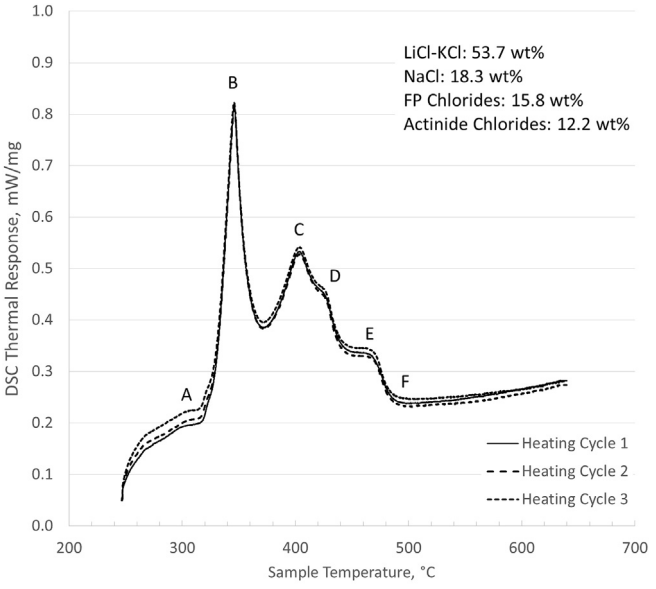

Fig. 4. DSC thermograms for simulant salt EBR-II B100. A) Onset: 317 °C. B) Peak 1: 346 °C. C) Peak 2: 403 °C. D) Peak 3: 426 °C. E) Peak 4: 469 °C. F) Liquidus: 483 °C.

shown in Fig. 5. At the beginning of FFTF fuel processing (FFTF B1), the Mk-IV ER salt is expected to have a liquidus temperature of 378 °C with an impurity concentration of 23.2 wt%. At the completion of EBR-II Mk-II fuel processing (EBR-II B165) (after 192 batches of fuel have been processed), the Mk-IV ER salt is expected to have a liquidus temperature of 512 °C with an impurity concentration near 55.1 wt%. The experimental results, based on the prediction of the MASTERS simulation, indicate that the liquidus temperature of the Mk-IV ER salt will have to be managed long before the final batch of fuel is processed.

The operating temperature of the Mk-IV ER is 500 °C. Superheat is the difference between the operating temperature and the liquidus temperature of salt. For example, if the operating temperature is 500 °C, and the liquidus temperature is 425 °C, then there is 75 °C of superheat. The data in Fig. 5 suggest that any spent fuel processed after EBR-II B25 would result in less than 75 °C superheat.

The onset temperature, liquidus temperature, enthalpy of fusion (upon cooling) of the nine simulant salts are listed in Table 8.

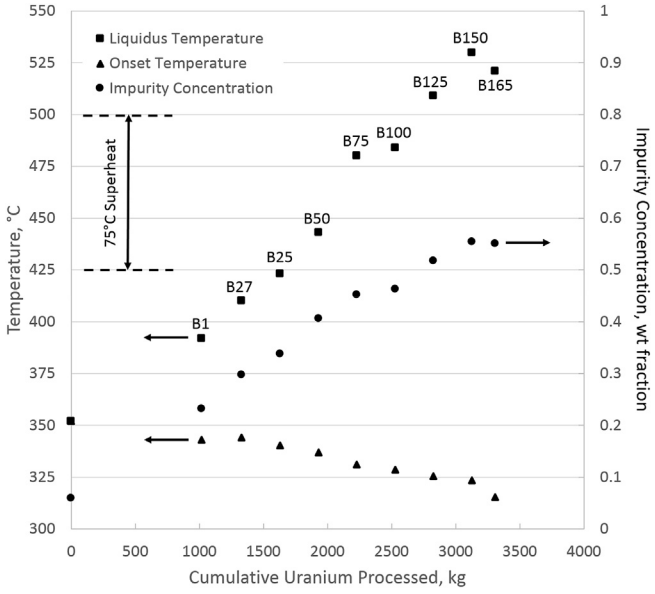

Fig. 5. Liquidus temperatures, onset temperatures, and impurity concentrations as a function of cumulative uranium processed.

4.3. Thermal property approximation with LiCl–KCl–NaCl system

Excluding the LiCl–KCl eutectic as the solvent salt, the NaCl concentration is greater than any other metal chloride in the simulant salts. Therefore, the NaCl concentration alone has a significant impact on the measured liquidus temperatures shown in Fig. 5. The compositions of the simulant salts were recalculated considering only LiCl, KCl, and NaCl. All other salt species are omitted from this exercise. The recalculated simulant salt compositions are listed in Table 9 along with the liquidus temperatures of the simulant salts, and the liquidus temperatures taken from phase diagram projections of the LiCl–KCl–NaCl salt system [27]. The data in Table 9 are presented graphically in Fig. 6.

The LiCl:KCl ratio remains constant for all data points representing the eutectic composition of LiCl–KCl (58-42 mol%). In the context of a ternary phase diagram, the abscissa in Fig. 6 represents varying NaCl concentration along the eutectic LiCl–KCl composition. That is, the composition at $x = 0$ is 100% LiCl–KCl eutectic, and the composition at $x = 1$ is 100% NaCl. The equations shown in Fig. 6 are effective when the mole fraction of NaCl is roughly between 0.1 and 0.35.

The two independent sets of liquidus temperatures summarized in Table 9 and shown in Fig. 6 are in close agreement with each

Table 8
Thermal measurements of the simulant salts.

Simulant Salt	Cycle	Onset Temperature, °C	Liquidus Temperature, °C	Enthalpy of Fusion, J/g
FFTF B1	1	342.9	378.9	−198.2
FFTF B27	1	342.7	391.8	−184.5
EBR-II B25	1	340.2	399.2	−202.4
	2	340.6	399.5	−203.6
	3	340.3	399.8	−203.7
	Average	340.4	399.5	−203.2
EBR-II B50	1	332.0	419.8	−168.4
	2	332.4	420.7	−166.6
	3	332.6	420.5	−165.5
	Average	332.3	420.3	−166.8
EBR-II B75	1	330.7	477.5	−175.9
	2	328.6	461.7	−177.3
	3	330.7	461.6	−174.4
	Average	330.0	466.9	−175.9
EBR-II B100	1	318.2	469.5	−182.7
	2	316.6	469.9	−179.8
	3	316.5	470.4	−177.6
	Average	317.1	469.9	−180.0
EBR-II B125	1	317.6	491.4	−170.6
	2	317.5	490.2	−175.9
	3	317.3	490.1	−172.3
	Average	317.5	490.6	−172.9
EBR-II B150	1	318.2	511.6	−199.6
	2	317.7	511.1	−177.0
	3	317.4	510.6	−185.6
	Average	317.8	511.1	−187.4
EBR-II B165	1	313.0	507.6	−213.2
	2	313.0	506.8	−210.2
	3	316.5	506.5	−209.4
	Average	314.2	507.0	−210.9

Table 9
Comparison of liquidus temperatures of simulant salts to the LiCl–KCl–NaCl ternary salt system.

Simulant Salt	KCl, wt%	LiCl, wt%	NaCl, wt%	Simulant Salt Liquidus Temperature,°C	LiCl–KCl–NaCl Liquidus Temperature [23],°C
FFTF B1	36.9	53.8	9.3	392	343
FFTF B27	36.1	52.7	11.2	410	405
EBR-II B25	35.1	51.0	13.9	423	420
EBR-II B50	33.1	48.2	18.7	443	450
EBR-II B75	31.2	45.4	23.3	480	480
EBR-II B100	30.8	44.8	24.4	483	485
EBR-II B125	29.0	42.1	28.9	509	515
EBR-II B150	27.2	39.5	33.2	530	535
EBR-II B165	27.6	40.1	32.3	521	530

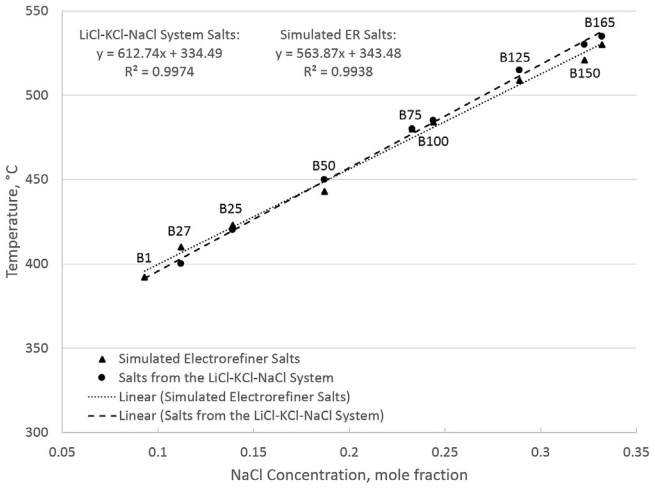

Fig. 6. Comparison of the simulant salt liquidus temperatures to the LiCl–KCl–NaCl ternary salt system.

other, with the exception of simulant salt FFTF B1. The LiCl–KCl–NaCl ternary salt system has a eutectic composition very close to the recalculated composition of simulant salt FFTF B1; 55-36-9 mol% and 53.8-36.9-9.3 mol%, respectively. The melting temperature of the eutectic composition is 346 ± 5 °C [27–29]. Because the recalculated composition of simulant salt FFTF B1 is, by coincidence, very close to the eutectic composition of the LiCl–KCl–NaCl ternary salt system, the comparison is skewed.

With the exception of FFTF B1, the concentration of NaCl in the ternary LiCl–KCl–NaCl system correlates with the measured liquidus temperature variations of the simulant salts with an error of ±5 °C. These results open the possibility for estimating the liquidus temperature of the Mk-IV ER salt (through the remaining EBR-II Mk-II fuel processing campaign) by considering only the concentrations of LiCl, KCl, and NaCl.

5. Conclusion

This study presented the measurement results of the liquidus temperatures of salt simulants representing the projected salt compositions of the Mk-IV ER during the processing campaigns of FFTF and EBR-II Mk-II fuels. It was determined that the liquidus temperature of the Mk-IV ER salt will increase as the concentrations of impurities (alkali, alkaline earth, and lanthanide fission products, transuranics, and sodium-bond) increase. Although this general trend was expected, the exact nature of the trend, as a function of type and mass of spent fuel processed, was neither quantified nor confirmed. This study is the first of its kind to investigate the effects of electrorefining operations on the thermal characteristics the of ER salt. With the results presented in this paper, given the 500 °C electrorefiner operation temperature, the recommendation is to manage the concentration of the metal chloride impurities in the salt in order to maintain 75 °C superheat. Considering the FFTF and EBR-II Mk-II fuels scheduled for processing, the Mk-IV ER salt is predicted to have less than 75 °C superheat after processing the entire inventory of 27 batches of FFTF fuel and 25 batches of EBR-II Mk-II fuel. The present work also indicates that the liquidus temperature of the MK-IV ER salt can be reasonably predicted by considering only the concentrations of LiCl, KCl, and NaCl.

Funding

The effort to prepare this manuscript was supported by the U.S. Department of Energy, Office of Nuclear Energy, Contract No. DEAC07-05ID14517.

Acknowledgements

The authors would like to thank Cynthia A. Adkins at the Idaho National Laboratory for her expertise and training on the operation of the Netzsch instrument. The experimental study was performed at INL by Toni Karlsson in support of her graduate studies at the University of Idaho [29]. Subsequently, Dr. Karlsson received a Ph.D. from Chalmers University of Technology, Department of Chemistry and Chemical Engineering in 2018.

Appendix A. Supplementary data

Supplementary data to this article can be found online at https://doi.org/10.1016/j.jnucmat.2019.04.016.

References

[1] C.E. Till, Y.I. Chang, Plentiful Energy: the Story of the Integral Fast Reactor, 2011. ISBN: 978-1466384606.
[2] Y.I. Chang, Integral fast reactor, Nucl. Technol. 88 (1989) 129–138.
[3] K.M. Goff, R.W. Benedict, S.G. Johnson, R.D. Mariani, M.F. Simpson, B.R. Westphal, Electrometallurgical Treatment Demonstration at ANL-West, American Nuclear Society Topical Meeting on DOE Spent Nuclear Fuel and Fissile Material Management, San Diego, CA, June 4-8, 2000.
[4] M.F. Simpson, K.M. Goff, S.G. Johnson, K.J. Bateman, T.J. Battisti, K.L. Toews, S.M. Frank, T.L. Moschetti, T.P. O'Holleran, W. Sinkler, A description of the ceramic waste form production process form the demonstration phase of the electrometallurgical treatment of EBR-II spent fuel, Nucl. Technol. 134 (2001) 263–277.
[5] Record of decision for the treatment and management of sodium-bonded spent nuclear fuel, department of Energy, Fed. Regist. 65 (182) (September 19, 2000) 56565–56570.
[6] D.E. Burkes, R.S. Fielding, D.L. Porter, D.C. Crawford, M.K. Meyer, A US perspective on fast reactor fuel fabrication technology and experience. Part I. Metal fuels and assembly design, J. Nucl. Mater. 389 (2009) 458–469.
[7] A.A. Madson, M.T. Laug, Xenon-Tagging of EBR-II Driver Fuel, Argonne National Laboratory, February 1972. Report ANL/EBR-057.
[8] S.X. Li, M.F. Simpson, Anodic process of electrorefining spent driver fuel in molten LiCl-KCl-UCl_3/Cd system, J. Miner. Metal. Process. 22 (2005) 192–198.
[9] B.R. Westphal, D. Vaden, S. Li, G. Fredrickson, R. Mariani, Fate of noble metal fission products during electrorefining, Proc. Global 2009 (September 6-11,

2009). Paris, France.
[10] D. Vaden, G.L. Fredrickson, Material control and accountability experience at the fuel conditioning facility, in: Proceedings of Global 2007, Boise, Idaho, September 9-13, 2007.
[11] T.S. Yoo, G.L. Fredrickson, D. Vaden, B. Westphal, Analysis of cadmium in undissolved anode materials of mark-IV electrorefiner, in: Proceedings of Global 2013, Salt Lake City, Utah, 2013.
[12] T.S. Yoo, D. Vaden, G.L. Fredrickson, B.R. Westphal, Analysis of undissolved anode materials of Mark_IV electrorefiner, J. Nucl. Mater. 510 (2018) 551–555.
[13] B.R. Westphal, S.M. Frank, W.M. McCartin, D.G. Cummings, J.J. Giglio, T.P. O'Holleran, P.A. Hahn, et al., Characterization of irradiated metal waste from the pyrometallurgical treatment of used EBR-II fuel, Metall. Mater. Trans. 46 (2015) 83–92.
[14] S. Li, T. Johnson, B. Westphal, M. Goff, R. Benedict, Electrorefining experience for pyrochemical reprocessing of spent EBR-II driver fuel, in: Proceedings of Global 2005, Tsukuba, Japan, October 9-13, 2005.
[15] D. Vaden, Fuel conditioning facility electrorefiner process model, Separ. Sci. Technol. 41 (2006) 2003–2012.
[16] Communication with T. S. Yoo Regarding Updated Modeling and Simulation of FFTF Fuel and EBR-II Mk-II Fuel Treatment Strategies.
[17] Communicatin with G. L. Fredrickson, T. S. Yoo, D. Vaden Regarding Treatment of FFTF U/Zr and EBR-II U/Fs Driver Fuels in the Mk-IV Electrorefiner.
[18] S. Zemczuzny, F. Rambach, Schmelzen der Alkalichloride, Z. Anorg. Chem. 65 (1910) 403–428.
[19] T.W. Richards, W.B. Meldrum, The melting points of the chlorides of lithium, rubidium and caesium, and the freezing points of binary and tenary mixtures of these salts, including also potassium and sodium chloride, J. Am. Chem. Soc. 39 (1917) 1816–1828.
[20] E. Elchagardus, P. Laffite, Etude Thermique des Systmes KCl-$BaCl_2$ et KCl-LiCl, Bull. Soc. Chim. de France: 51 (1932) 1572–1579.
[21] E. Korin, L. Soifer, Thermal analysis of the system KCl-LiCl by differential scanning ccalorimetry, J. Therm. Anal. 50 (1997) 347–354.
[22] A. Basin, A. Kaplun, A. Meshalkin, N. Uvarov, The LiCl-KCl binary system, Russ. J. Inorg. Chem. 53 (2008) 1509–1511.
[23] M. Temkin, Mixtures of fused salts as ionic solutions, Acta Physicochim. 20 (1945) 411–420.
[24] M.W. Chase, C.A. Davis, J.R. Downey, D.J. Frurip, R.A. McDonald, A.N. Syverud, JANAF thermochemical tables, Third Edition, J. Phys. Chem. Ref. Data 14 (Sup. 1) (1985).
[25] C. Solomons, J. Goodkin, H.J. Gardner, G.J. Janz, Heat of fusion, entropy of fusion and cryoscopic constant of the LiCl–KCl eutectic mixture, J. Phys. Chem. 62 (1958) 248–249.
[26] A.S. Dworkin, M.A. Bredig, The heat of fusion of the alkali metal halides, J. Phys. Chem. 64 (1960) 269–272.
[27] J. Sangster, A.D. Pelton, Thermodynamic calculation of phase diagrams of the 60 common-ion ternary systems containing cations Li, Na, K, Rb, Cs and anions F, Cl, Br, I, J. Phase Equilibria 12 (1991) 511–537.
[28] E.K. Akopov, A.G. Bergman, The K, Li, Na || Cl syste, Russ. J. Inorg. Chem. 11 (1966) 7.
[29] T.Y. Gutknecht, Thermal Analysis of Surrogate Molten Salts with Metal Chloride Impurities for Electrorefining Used Nuclear Fuel, Thesis for the Degree of M.Sc. Nuclear Engineering, University of Idaho, April 24, 2012.